J. Biochem. 2009;146(6)787–796
doi:10.1093/jb/mvp124

Possible Role of Mitochondrial Remodelling on Cellular Triacylglycerol Accumulation

Toshiyuki Kita[1], Hana Nishida[1], Hirofumi Shibata[1], Shingo Niimi[2], Tomihiko Higuti[1] and Naokatu Arakaki[1,*]

[1]Department of Molecular Cell Biology and Medicine, Institute of Health Bioscience, The University of Tokushima Graduate School, Tokushima 770-8505; and [2]Division of Biological Chemistry and Biologicals, National Institute of Health Sciences, Kamiyoga, Tokyo 158-8501, Japan

Received May 1, 2009; accepted July 27, 2009; published online August 10, 2009

Mitochondrial fusion and fission processes play a role in a variety of cell functions, including energy metabolism, cell differentiation and programmed cell death. Still, it is not clear how these processes contribute to the cell functions. Here, we investigated the role of mitochondrial remodelling on lipid metabolism in adipocytes. In 3T3-L1 pre-adipocytes, the morphology of mitochondria is organized as a continuous reticulum. Upon differentiation of adipocytes manifested by cellular triacylglycerol (TG) accumulation, mitochondrial morphology altered from filamentous to fragmented and/or punctate structures. When the mitochondrial fusion was induced in adipocytes by silencing of mitochondrial fission proteins including Fis1 and Drp1, the cellular TG content was decreased. In contrast, the silencing of mitochondrial fusion proteins including mitofusin 2 and Opa1 increased the cellular TG content followed by fragmentation of mitochondria. It also appears that polyphenolic phytochemicals, negative regulators of lipid accumulation, have mitochondrial fusion activity and that there is a good correlation between mitochondrial fusion activity and the cellular TG accumulation-reducing activity of the phytochemicals. These results suggest that cellular TG accumulation is regulated, at least in part, via mitochondrial fusion and fission processes.

Key words: adipocytes, fission, fusion, mitochondria, phytochemicals, triacylglycerol.

Abbreviations: DMSO, dimethylsulphoxide; dsRNAs, double-stranded RNAs; GAPDH, glucose-6-phosphate dehydrogenase; Mfn2, mitofusin2; OA, oleic acid; PBS, Mg^{2+}- and Ca^{2+}-free phosphate-buffered saline; RNAi, RNA interference; TFP, mitochondrial tube formation potential; TG, triacylglycerol.

Mitochondria are highly dynamic organelles and undergo continuous fission and fusion events in physiological situations (*1*, *2*). Defined sets of proteins have been known to mediate mitochondrial fission and fusion, and to constitute regulatory components controlling mitochondrial dynamics (*3–8*). Recent work indicates that maintaining mitochondrial morphology is critical to normal cell function. For example, mammalian cells lacking mitochondrial fusion grow slowly due to low respiratory capacity (*6*) and mice deficient in mitochondrial fusion die early in development (*5*), whereas yeast mitochondrial fusion mutants rapidly lose their mitochondrial DNA (*7*). Moreover, mutations in gene-encoding fusion proteins have been implicated in human neurodegenerative diseases: mitofusin 2 (Mfn2) in peripheral neuropathy Charcot–Marie-Tooth Disease subtype 2A and OPA1 in autosomal dominant optic atrophy (*9–12*). Recent work has also indicated that mitochondrial fusion and fission processes play a role in cell survival and programmed cell death (*13–19*). Interestingly, it was shown that CED-9, the *Caenorhabditis elegans* Bcl-2 homolog, when ectopically expressed in HeLa cells can interact with Mfn2 and induce mitochondrial fusion and that Bax and Bak are involved in the regulation of mitochondrial fusion through interactions with Mfn2 in healthy cells (*20*, *21*).

In addition, there is substantial evidence that proteins participating in mitochondrial fusion or fission also have a role in metabolism. Bach *et al*. (*22*) reported that stably transfected fibroblasts with an Mfn2 antisense sequence show reduced glucose oxidation and a similar reduction in oxygen consumption. Mfn2 repression is also associated with decreased rates of pyruvate or palmitate oxidation in L6E9 muscle cells (*22*, *23*). These data suggest that the mitochondrial network *per se* or proteins that participate in the generation of the mitochondrial network may be involved in the control of mitochondrial energy metabolism. However, the role of mitochondrial remodelling on metabolism of lipid and carbohydrate is poorly understood.

In this study, we investigated the role of mitochondrial remodelling on triacylglycerol (TG) accumulation in adipocytes and found that mitochondrial morphology alters from filamentous to fragmented and/or punctate structures during adipocyte differentiation. We also found that the induction of mitochondrial fusion causes a decrease in cellular TG accumulation, while the induction of mitochondrial fission causes an increase in cellular TG accumulation. Finally, we showed that many

*To whom correspondence should be addressed. Tel: +81-88-633-7255, Fax: +81-88-633-9550,
E-mail: arakaki@ph.tokushima-u.ac.jp

phytochemicals, negative regulators of cellular TG accumulation in adipocytes (*24*), have mitochondrial fusion activity. This is the first report investigating the role of mitochondrial remodelling on adipocyte differentiation, and the present results indicate that mitochondrial fusion and fission processes govern lipid metabolism in adipocytes.

MATERIALS AND METHODS

Cell Culture and Differentiation—Murine 3T3-L1 pre-adipocytes were maintained in a Dulbecco's modified Eagle's medium (DMEM) (Wako Pure Chemical Industries Ltd, Osaka, Japan) with 10% (v/v) fetal calf serum (Equitech-Bio Inc., Cotton Gin Lane Kerrville, TX, USA) and antibiotics in a humidified atmosphere of 95% air and 5% CO_2 at 37°C. Differentiation was induced by incubating the confluent preadipocytes in adipogenic medium (2 μM insulin, 1 μM dexamethasone and 250 μM isobutylmethylxanthine in DMEM) (day 0) for 2 days, followed by changing of the medium (every 2 days) containing 2 μM insulin for another 16 days.

Morphological Analysis of Mitochondria and Endoplasmic Reticulum—The cells (day 0 and day 8) were stained and incubated with 250 nM MitoTracker Green FM or 1μM ER-Tracker Green (Molecular Probes, Eugene, OR, USA) for 30 min at 37°C in a 5% CO_2 incubator. After staining, the cells were washed twice with phosphate-buffered saline (PBS), and fresh medium was added; the cells were then observed under fluorescent microscopy (1000× magnification) (OLYMPUS IX70, OLYMPUS, Tokyo, Japan). We also gained 3D images for each cell by using Z-slice and 3D reconstruction (Fig. 1).

Evaluation of Mitochondrial Tube Formation Potential—3T3-L1 pre-adipocytes (day 0) were incubated with 0.1% dimethylsulphoxide (DMSO) as a control and the indicated concentrations of phytochemicals for 48 h. The cells were stained and incubated with 250 nM MitoTracker Green FM. After staining, the cells were

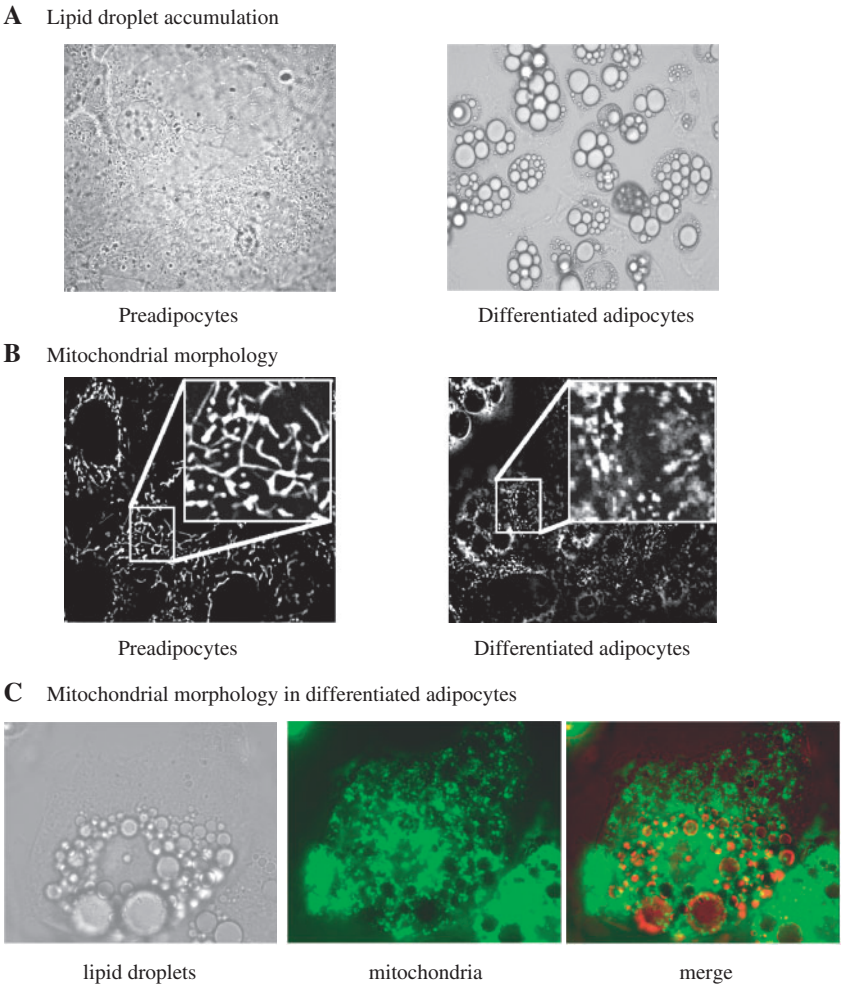

Fig. 1. **Morphological changes in mitochondria after adipocyte differentiation.** Differentiation of 3T3-L1 pre-adipocytes was induced by incubating them in adipogenic medium, and lipid droplets (A) and mitochondrial morphology (B) were determined in differentiated adipocytes (Day 16) and pre-adipocytes, respectively, as described in MATERIALS AND METHODS section. White signals observed in (B) showed mitochondria. (C) Lipid droplets and mitochondria were stained with Oil Red O and MitoTracker Green, respectively, and merged images of mitochondria and lipid droplets were shown.

washed twice with PBS, and fresh medium was added; the cells were then observed under fluorescent microscopy (1000× magnification). We then defined the mitochondrial morphology as follows: (i) granule type (≤1 μm in length), (ii) short type (1–2 μm in length), (iii) medium type (2–5 μm in length), (iv) long type (≥5 μm in length) and (v) highly tubular type (≥5 μm in length and seemed just like one web networks). In addition, we scored mitochondrial morphology in each cell as follows; if over the 50% of mitochondria in one cell showed granule type structure (≤1 μm in length), the score was defined as −1. If over the 50% of mitochondria in one cell showed short type, scores of those cells were defined as score +1. Similarly, if over the 50% of mitochondria in one cell showed medium, long and highly tubular, scores of those cells were defined as score +2, +3 and +5, respectively. The total score (mitochondrial tube formation potential: TFP) was evaluated from the sum of ∼50 cells' scores.

Oil Red O Staining—3T3-L1 adipocytes (day16) were incubated with each sample for 48 h and then fixed by 3.7% formalin in PBS, washed once with 60% isopropanol and then stained with Oil Red O for 1 h at 37°C in a 5% CO_2 incubator. The stained cells were washed once rapidly with xylene, and then extracted with 600 ml of 99.5% ethanol. The extracts were stored at −20°C, and 10 ml of each extract was added to 90 ml of 99.5% ethanol; the absorbance was then read in the spectrophotometric plate reader at 490 nm.

RNA interference and Transfection—Double-stranded RNAs (dsRNAs) for Fis1, Mfn2, Drp1 and OPA1 were designed and synthesized by Nippon EGT (Toyama, Japan). The sequences of the dsRNAs used were shown in Table 1. dsRNAs for human GAPDH, hMfn2 and hDnm1 were kindly gifted from Drs Masamichi Kuwajima (Kaisei General Hospital, Kagawa, Japan) and Akiko Sukeno (Departmen of Nutritional Physiology, Institute of Health Biosciences, The University of Tokushima Graduate School, Tokushima, Japan). 3T3-L1 preadipocytes (day 0) and adipocytes (day 16) cultured on the glass-bottomed dishes were transfected with 50 nM dsRNAs using Lipofectamine 2000 (Invitrogen, Carlsbad, CA, USA) according to the manufacturer's protocol. Two days after transfection, adipocytes were incubated with 250 nM MitoTracker Green FM for 30 min, and the mitochondrial morphology was observed under fluorescent microscopy. The TFP levels were then calculated as described above. Transfection of dsRNAs resulted in a dose-dependent inhibition of mRNA expression and 50 nM dsRNA showed maximal inhibitory effects (data not shown).

Table 1. **Sequences of dsRNAs.**

Gene	Sequence
Mouse Fis1 (sense)	5′-UGAAAAGGCUCUAAAGUAUdTdT-3′
Mouse Fis1 (antisense)	3′-dTdTACUUUUCCGAGAUUUCAUA-5′
Mouse Mfn2 (sense)	5′-ACAUCUUCAUCCUGAACAAdTdT-3′
Mouse Mfn2 (antisense)	3′-dTdTUGUAGAAGUAGGACUUGUU-5′
Mouse Opa1 (sense)	5′-ACAGGCUGAUAGUUUUAAAdTdT-3′
Mouse Opa1 (antisense)	3′-dTdTUGUCCGACUAUCAAAAUUU-5′
Mouse Drp1 (sense)	5′-UGAGUAUGCUUUUCUUCAAdTdT-3′
Mouse Drp1 (antisense)	3′-dTdTACUCAUACGAAAAGAAGUU-5′
Human Mfn2 (sense)	5′-ACAUCUUCAUCCUGAACAATT-3′
Human Mfn2 (antisense)	5′-UUGUUCAGGAUGAAGAUGUTT-3′
Human Dnm1 (sense)	5′-GAAGAAUUUUCCCGCUUUATT-3′
Human Dnm1 (antisense)	5′-UAAAGCGGGAAAAUUCUUCTT-3′

Western Blot Analysis—The cells treated with dsRNAs for 2 days were washed with PBS, collected and then lysed in RIPA buffer (10 mM Tris–HCl, pH 7.4, 5 mM EDTA, 150 mM NaCl, 1% Triton X-100, 10 μg/ml leupeptin, 0.1 trypsin inhibitor unit/ml aprotinin, 1 mM vanadate, and 100 mM NaF). Cell lysates were resolved by SDS–PAGE and subjected to western blotting. Membranes were incubated with anti-Mfn2, anti-Drp1, anti-Opa1 antibodies for 1 h at room temperature, and then they were incubated with a horseradish peroxidase-conjugated anti-mouse or anti-rabbit IgG antibodies. Protein bands were visualized by enhanced chemiluminescence (ECL; Amersham Pharmacia Biotech, Buckinghamshire, UK), according to the manufacturer's instructions. Anti-rabbit Mfn2 antibody which react with mouse Mfn2 was obtained from Sigma (St Louis, MO, USA) and anti-human Drp1 and Opa1 antibodies which react with mouse Drp1 and Opa1 were from BD Transduction Laboratories (San Diego, CA, USA).

RNA extraction and RT–PCR—For total RNA preparation, culture media were removed and the cells were washed twice with PBS and lysed in TRIZOL Reagent (Invitrogen). RNA was purified according to the manufacturer's instructions. Synthesis of cDNA from the isolated total RNA was carried out using M-MLV reverse transcriptase (Promega). A reverse transcription mixture was amplified by PCR using GoTaq Green Master Mix (Promega) in the presence of 0.5 mM sense and antisense primers, as described below. For mouse Mfn 2 (product size: 208 bp); sense primer (5′-GCCAGCTTCCTTGAAGA CAC-3′) and antisense primer (5′-GCAGAACTTTGTCCC AGAGC-3′), for mouse Mfn 1 (195 bp); sense primer (5′-GCTGTCAGAGCCCATCTTTC-3′) and antisense primer (5′-CAGCCCACTGTTTTCCAAAT-3′), for mouse Fis 1 (776 bp); sense primer (5′-CCTTAGTGTGAGGCTT TCAGG-3′) and antisense primer (5′-GGCAGAGAGCAG GTGAGG-3′), for mouse GAPDH; sense primer (5′-AACT TTGGCATTGTGGAAGG-3′) and antisense primer (5′-ACACATTGGGGGTAGGAACA-3′), for mouse Drp 1 (180 bp); sense primer (5′-ATGCCTGTGGGCTAATGA AC-3′) and antisense primer (5′-AGTTGCCTGTTGTTGG TTCC-3′), for mouse Opa 1 (187 bp); sense primer (5′-GATGACACGCTCTCCAGTGA-3′) and antisense primer (5′-TCGGGGCTAACAGTACAACC-3′), for human GAPDH (238 bp); sense primer (5′-GAGTCAACGGATTT GGTCGT-3′) and antisense primer (5′-TTGATTTTGGAG GGATCTCG-3′), for human Mfn2 (169 bp): sense primer (5′-GACCCCGTTACCACAGAAGA-3′) and antisense primer (5′-GCAGAACTTTGTCCCAGAGC-3′), for human Dnm1 (208 bp): sense primer (5′-TGATGTGCTGGAGAAC AAGC-3′) and antisense primer (5′-CGTCAGTTGCTGAT TGAGGA-3′) were used.

Statistical Analysis—Experimental and control samples used in the functional assays were compared for statistical significance using the Student's *t*-test. $P < 0.05$ was considered as statistically significant.

RESULTS

Mitochondrial Morphological Dynamics in Adipocytes—3T3-L1 pre-adipocyte is one of the most well-characterized and reliable models for studying adipogenesis. Treatment with adipogenic agents induces a program of differentiation manifested by large lipid droplet accumulation, as shown in Fig. 1A. To determine the physiological role of mitochondrial remodeling on lipid metabolism, we first investigated the morphological change of mitochondria during adipocyte differentiation. As shown in Fig. 1B, mitochondrial morphology is organized as a continuous reticulum in 3T3-L1 pre-adipocyte. Upon differentiation of adipocytes, however, mitochondrial morphology altered from filamentous to fragmented and/or punctate structures, suggesting that mitochondrial remodelling plays a role in adipocyte differentiation. It is possible that mitochondrial morphology was artificially affected by the accumulated lipid droplets as reported by Stone *et al*. (*25*), but as shown in Fig. 1C, mitochondria were not co-localized with lipid droplets, indicating that mitochondrial morphology was not artificially affected by the accumulated lipid droplets.

Role of Mitochondrial Remodelling on Cellular TG Accumulation—Mitochondrial morphological dynamics are determined by a balance between two opposing processes, fission and fusion (*2*, *7*). Knock down of mitochondrial fusion and fission genes induces mitochondrial fragmentation and fusion, respectively. To determine whether mitochondrial remodelling is involved in adipocyte differentiation, we examined the effects of dsRNAs for mitochondrial remodelling genes on cellular TG accumulation (adipocyte differentiation marker). Transfection of dsRNA for Drp1, a mitochondrial fission protein, caused suppression of Drp1 expression by ~70% (Fig. 2C) and induced long tubular mitochondrial (Fig. 2A and B) in 3T3-L1 adipocytes. As we expected, silencing of Drp1 caused a decrease in the cellular TG content by ~35% (Fig. 2D). We next examined the effect of silencing of Mfn2, a mitochondrial fusion protein, on the cellular TG content in 3T3-L1 pre-adipocytes. As shown in Fig. 2C, transfection of dsRNA for Mfn2 in 3T3-L1 pre-adipocytes caused a 30–45% suppression of Mfn2 expression, followed by fragmentation of mitochondria (Fig. 2A and B), and resulted in an increase in the cellular TG content (Fig. 2D). Two protein bands with molecular weight of 86 kDa and 68 kDa were recognized with a polyclonal antibody against Mfn2 used in this study. The relative values of these two bands (in arbitrary units), normalized for differences in loading, were decreased in dsRNA-treated cells (30 and 45% decrease, respectively). Although the nature of two protein bands is not clear at present, these two bands seems to be Mfn2 itself or closely related proteins in which two forms of Mfn2 were also reported in differentiated L6E9 myotube cells (*26*). Furthermore, we investigated a role of other mitochondrial remodelling proteins such as Fis1, a mitochondrial fission protein, and Opa1, a mitochondrial fusion protein, on cellular TG accumulation. As shown in Fig. 2D, silencing of Fis1 resulted in a decrease in the cellular TG content, while silencing of Opa1 resulted in an increase in the cellular TG content. We observed that silencing of Opa1 and Fis1 caused a 40–45% suppression of mRNA expression of Opa1 and Fis1, respectively, followed by induction of mitochondrial fragmentation and fusion, respectively (data not shown). Although we could not determine the protein level of Fis1 and Opa1 in adipocytes, these results suggest that mitochondrial fusion and fission processes are involved, at least in part, in the regulation of cellular TG accumulation.

Phytochemicals have Mitochondrial Fusion Activity—We have recently reported that phytochemicals, including resveratrol, piceatannol and kaempferol, inhibit cytosolic lipid droplet accumulation in adipocytes (also shown in Fig. 3A), probably via inhibition of cell-surface H^+-ATP synthase (*24*, *28*). Since induction of mitochondrial fusion causes a decrease in cellular TG accumulation, as described earlier, these phytochemicals can be expected to have mitochondrial fusion activity. To prove this, we examined the effects of these substances on mitochondrial morphology using 3T3-L1 pre-adipocytes because mitochondrial morphology can be easily observed in pre-adipocytes than in differentiated adipocytes under a fluorescent microscope. When pre-adipocytes were treated with phytochemicals including piceatannol, resveratrol and kaempferol, the formation of filamentous network structures of mitochondria was stimulated (Fig. 3B). Then, we further investigated the effects of a variety of phytochemicals (over 50 samples) on cellular TG accumulation and mitochondrial morphology. As shown in Fig. 3C, there was a good correlation between mitochondrial fusion activity and cellular TG accumulation-reducing activity of the phytochemicals, confirming that mitochondrial fusion and fission processes play a role in the regulation of cellular TG accumulation. Furthermore, we recently found that mitochondrial fragmentation can be observed in non-adipocyte HeLa cells by treating the cells with oleic acid (OA). As shown in Fig. 4, treatment of the cells with 500 μM OA induced mitochondrial fragmentation followed by increase in intracellular lipid content as compared to control cells. Interestingly, resveratrol dose-dependently induced mitochondrial fusion in OA-treated HeLa cells followed by reduction of cellular TG accumulation (Fig. 4B and Table 2). Resveratrol was effective at 10 μM and the effects of resveratrol were observed within 3 h treatment. More interestingly, we found that knockdown of human Mfn2 increased cellular TG content, while knockdown of human Dnm1 (human mitochondrial fission protein) decreased cellular TG content in HeLa cells (Fig. 4C).

DISCUSSION

The present results strongly suggest that mitochondrial fusion and fission processes play a role in cellular TG accumulation. It also appears that polyphenolic phytochemicals, negative regulators of lipid accumulation, have mitochondrial fusion activity and that there is a good correlation between mitochondrial fusion activity and the cellular TG accumulation-reducing activity of the phytochemicals, thus confirming that mitochondrial fusion governs cellular TG accumulation. Mitochondrial remodeling can be observed in non-adipocyte cells

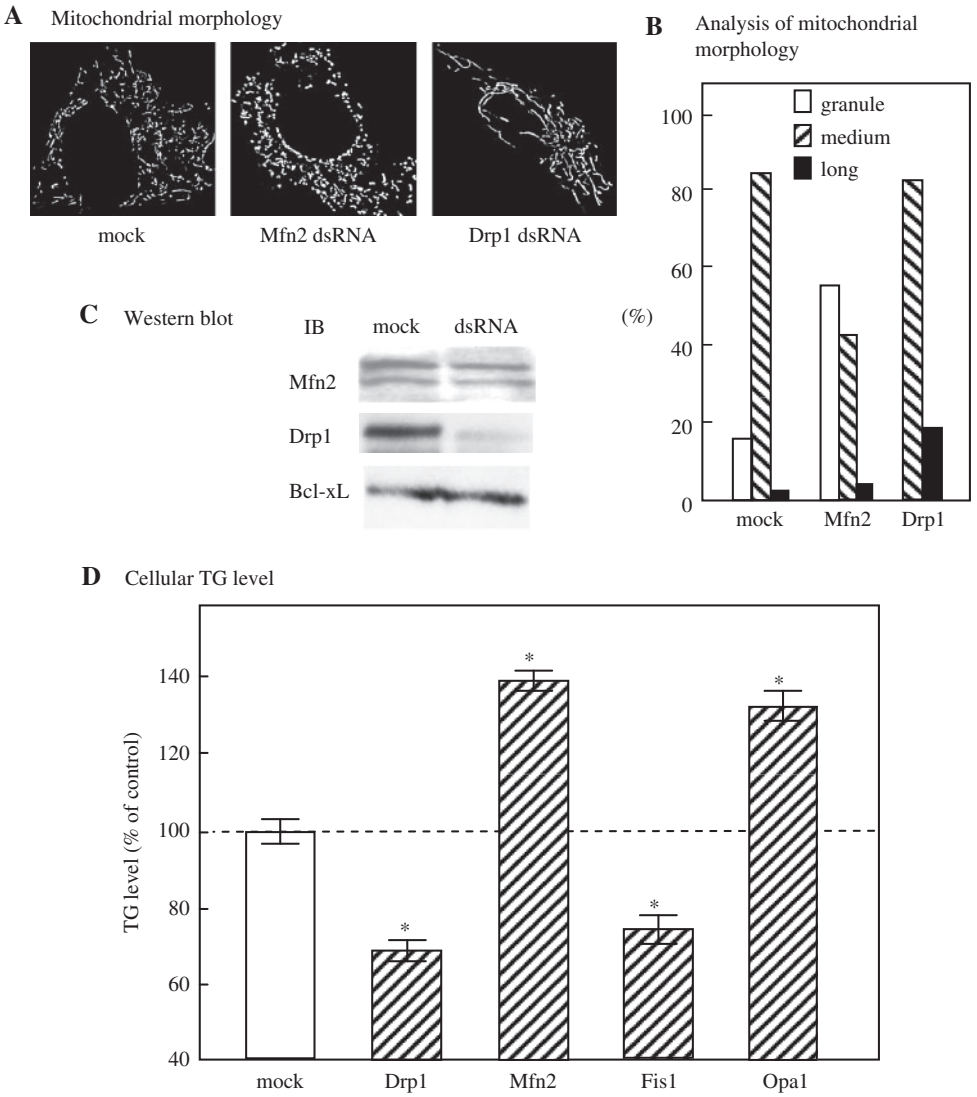

Fig. 2. **Cellular TG accumulation and mitochondrial morphology in mitochondrial remodeling gene-silenced cells.** (A) 3T3-L1 adipocytes were transfected with 50 nM of dsRNAs for Mfn2 and Drp1. Two days after transfection, the cells were observed under fluorescent microscopy. (B) For the quantification of mitochondrial morphology in dsRNA-treated cells, we counted at least 200 cells in each experiments and then the cells were grouped into three categories, class 1 with granule type mitochondria (<1 μm in length), class 2 with medium type mitochondrial rods (<5 μm in length) and class 3 with long-type mitochondria (>5 μm in length). The number of cells with the indicated mitochondrial morphology is shown as a percentage of the total number counted. (C) The expression of Mfn2, Drp1 and Opa1 in mock- and dsRNA-transfected cells were determined by western blotting. The expression of Bcl-xL was used as a loading control and the relative values of these protein bands (in arbitrary units), normalized for differences in loading, were determined. The data are representative of two independent experiments that gave similar results. (D) 3T3-L1 adipocytes were transfected with 50 nM of dsRNAs for Mfn2, Drp1, Fis1 and Opa1. Two days after transfection, cellular TG content in dsRNA-treated cells was determined as described in MATERIALS AND METHODS section. The results shown are the mean ± SEM of three independent experiments. Asterisk indicates the significance different compared with mock control cells, $P < 0.01$.

including HeLa cells in which OA added extracellularly induced mitochondrial fragmentation accompanied with the increase in intracellular lipid content. Interestingly, resveratrol induced mitochondrial fusion in OA-treated HeLa cells followed by reduction of TG accumulation in the cells. We also found that knockdown of human Mfn2 increased cellular TG content, while knockdown of human Dnm1 (human mitochondrial fission protein) decreased cellular TG content in HeLa cells. These results also suggest that mitochondrial fission and fusion activities are changed under the physiological (*e.g.* adipocyte differentiation) and pathological (*e.g.* excessive intake of lipids) conditions. To our knowledge, this is the first report indicating the direct role of mitochondrial fusion and fission processes on the regulation of cellular TG accumulation in adipocytes.

Although the mechanism of regulation of cellular TG accumulation by induction of mitochondrial fusion remains to be determined, it has been suggested that mitochondria are capable of more rapidly supplying

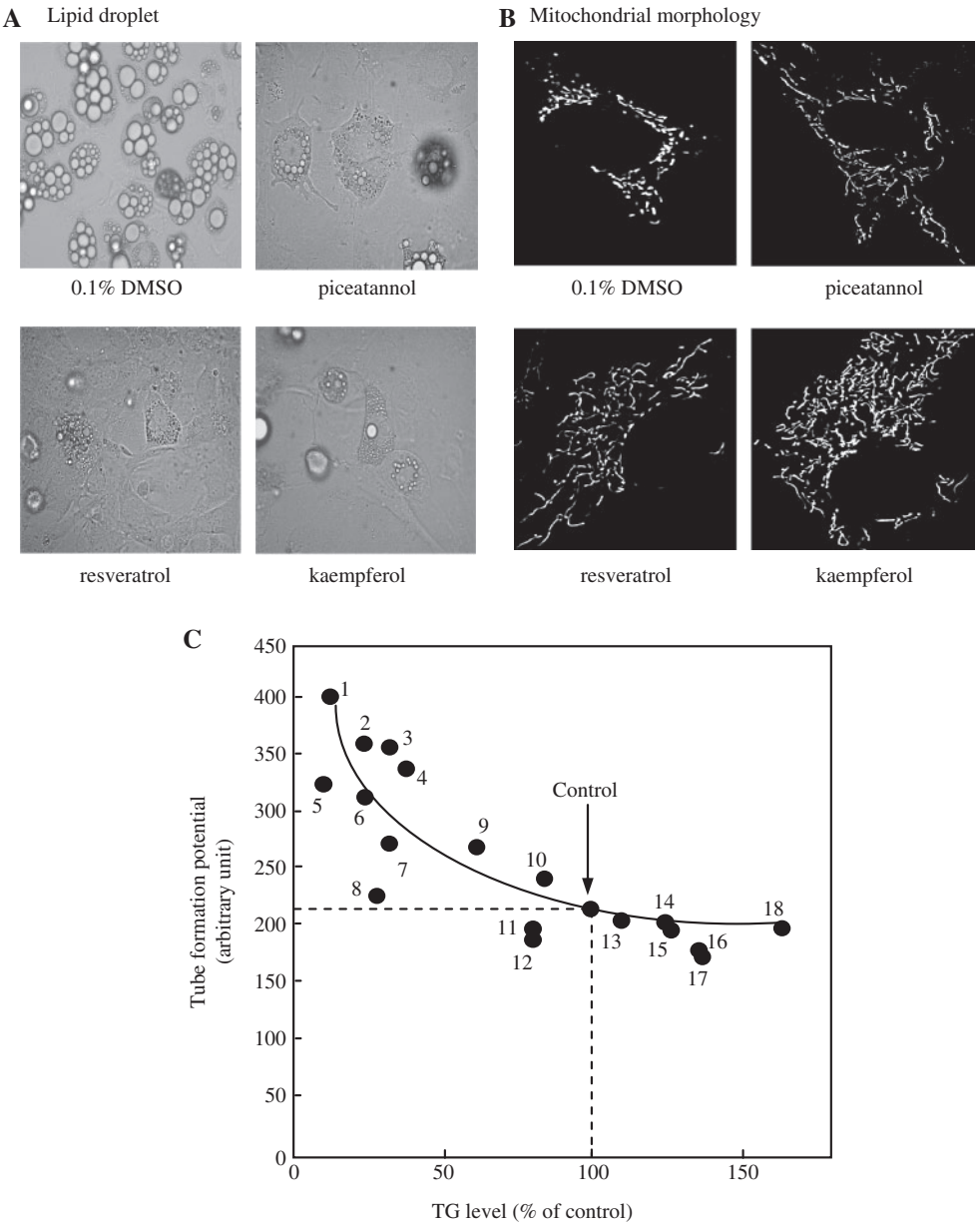

Fig. 3. **Effects of phytochemicals on cellular TG accumulation and mitochondrial morphology.** 3T3-adipocytes were incubated with or without resveratrol (50 μM), piceatannol (10 μM), kaempferol (60 μM) for 48 h. Cytosolic lipid droplets (A) and mitochondrial morphology (B) were visualized under a phase-contrast microscope and fluorescent microscope, respectively, as described in MATERIALS AND METHODS section. (C) 3T3-L1 pre-adipocytes (day0) were incubated with 0.1% DMSO as a control, 1; 50 μM resveratrol, 2; 60 μM kaempferol, 3; 130 μM daidzein, 4; 60 μM genistein, 5; 55 μM apigenin, 6; 10 μM piceatannol, 7; 20 μM luteolin, 8; 50 μM quercetin, 9; 20 μM rosmarinic acid, 10; 20 μM EGC, 11; 50 μM EC, 12; 70 μM phloretin, 13; 20 μM quercitrin, 14; 20 μM taxifolin, 15; 20 μM EGCG, 16; 50 μM ECG, 17; 20 μM naringenin, 18; 20 μM naringin each for 48 h. After incubation, mitochondrial morphology and TFP in the cells were determined as described in MATERIALS AND METHODS section. For the analysis of cellular TG levels, differentiated adipocytes were incubated with or without phytochemicals as described above for 48 h and then cellular TG levels were determined as described in MATERIALS AND METHODS section. Note that sample numbers 1, 2, 3, 4, 5, 6, 8 and 10 were shown to inhibit H^+-ATP synthase and that the concentrations of phytochemicals were IC_{50} of the phytochemicals for purified H^+-ATP synthase (except for apigenin) (*27*). The results shown are the means of two independent experiments.

ATP to the intracellular organelles such as nuclei according to the energy requirement in the organelles as intracellular power-transmitting cables (*29*). In addition, mitochondria ensure metabolite and mitochondrial DNA mixing, and are involved in metabolism of lipids, amino acids and nucleotides, and in ion homeostasis. Thus, it can be speculated that extended reticular networks of mitochondria might be capable of more efficiently performing pyruvate dehydrogenation, oxidative phosphorylation and metabolism of lipids and amino acids, and that

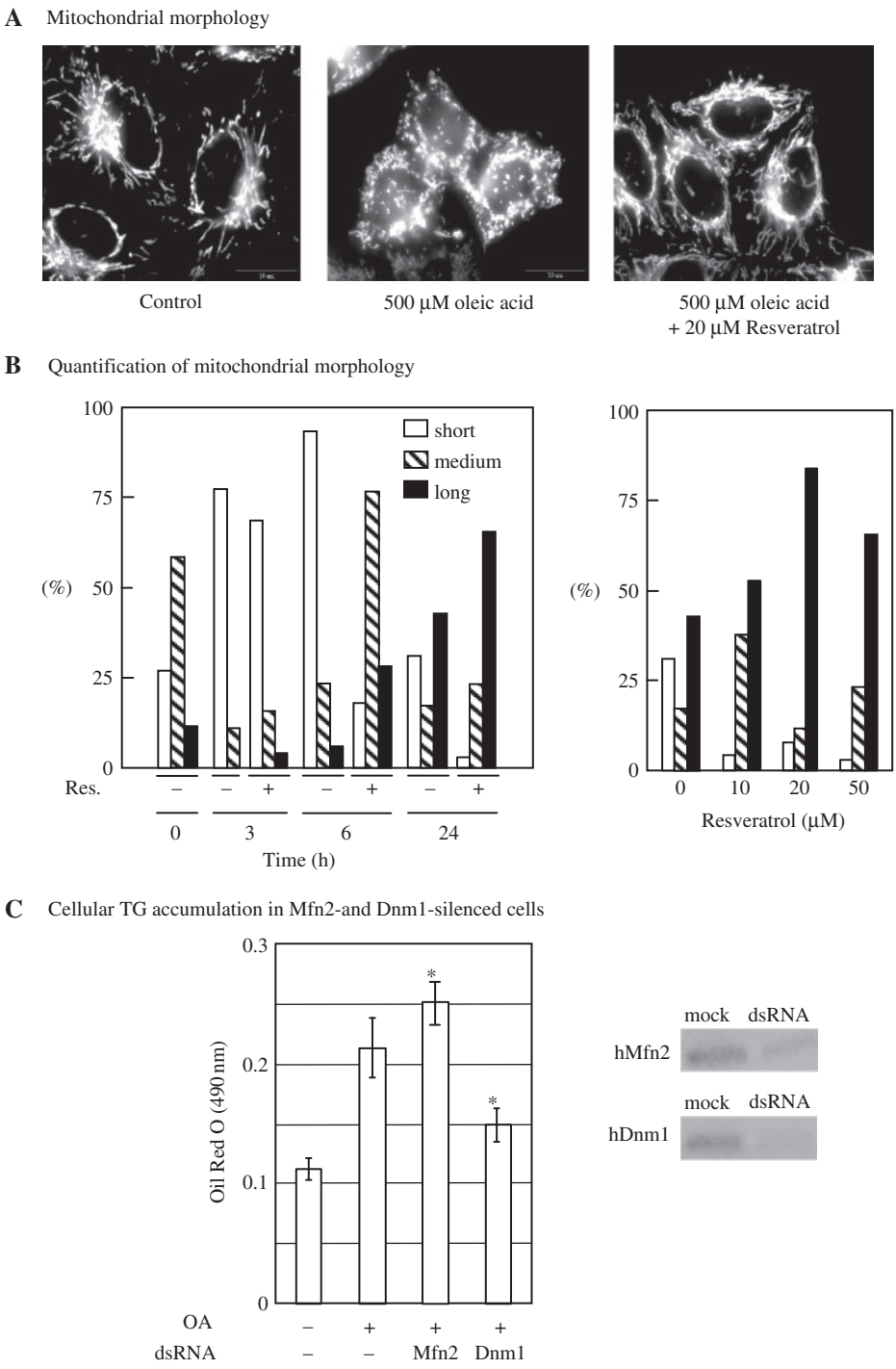

Fig. 4. **Effect of resveratrol on cellular TG accumulation and mitochondrial morphology in OA-treated HeLa cells.** (A) HeLa cells were treated with 500 μM of OA for 24 h and then incubated with or without 20 μM of resveratrol for 24 h. Mitochondrial morphology was determined as described in MATERIALS AND METHODS section. The data shown are representative of two independent experiments. (B) (Left) HeLa cells treated with 500 μM of OA for 24 h were incubated for 3 h, 6 h and 24 h in the presence or absence of 50 μM of resveratrol. Quantification of mitochondrial morphology was determined as described in MATERIALS AND METHODS section. The data shown are the means of two independent experiments. (Right) HeLa cells treated with 500 μM of OA for 24 h in the presence or absence of indicated concentrations of resveratrol (Res), and then mitochondrial morphology was determined. The data shown are the means of two independent experiments. The number of cells with the indicated mitochondrial morphology is shown as a percentage of that total number counted. (C) HeLa cells were transfected with 50 nM of dsRNAs for human Mfn2 and human Dnm1 (human mitochondrial fission protein). Two days after transfection, cellular TG content in dsRNA-treated cells was determined as described in MATERIALS AND METHODS section. Treatment of the cells with dsRNA caused downregulation of targeted proteins by 60–80%, but not GAPDH (data not shown). $^{*}P < 0.05$ vs. OA treatment.

Table 2. **Effect of resveratrol on cellular TG accumulation in OA-treated HeLa cells.**

Incubation time (h)	OA	Resveratrol (μM)	TG (OD at 490 nm)
0	–	0	0.20
3	+	0	0.50
3	+	10	0.47
3	+	20	0.29
3	+	50	0.38
6	+	0	0.54
6	+	50	0.25
24	+	0	0.60
24	+	50	0.36

HeLa cells were treated with 500 μM OA for 24 h and then incubated with or without indicated concentrations of resveratrol for 3 h, 6 h and 24 h. Cellular TG levels were determined as described in MATERIALS AND METHODS section. The results shown are the means of two independent experiments.

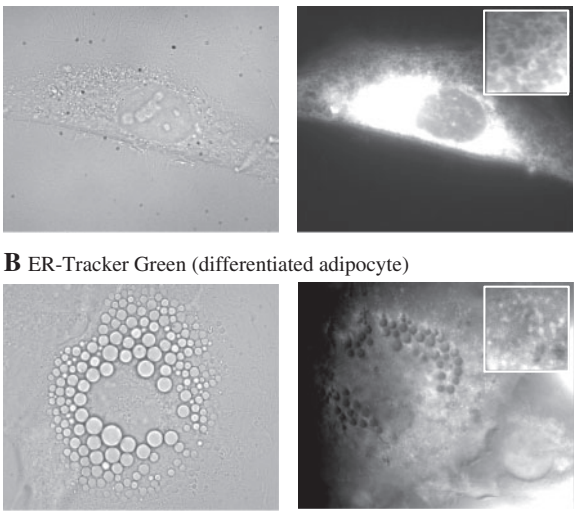

Fig. 5. **Morphology of ER in adipocyte.** Morphology of ER was determined as described in MATERIALS AND METHODS section in 3T3-L1 pre-adipocytes (A) and differentiated adipocytes (B). Note that induction of adipocyte differentiation caused alteration of morphology of ER from filamentous to fragmented and/or punctate structures.

dysregulated mitochondrial morphology might cause dysfunctions of oxidative phosphorylation and lipid metabolism. Moreover, it is also well known that nuclear genome has a leading role in the biogenesis of mitochondrial respiratory chain and that nuclear activity can be modulated by signals sent by mitochondria (*30–32*), suggesting that dysregulated mitochondrial morphology could alter gene expression of proteins involved in lipid metabolism. We are now trying to identify up- or down-regulated genes in mitochondrial remodeling gene-silenced cells. On the other hand, it has been reported that fatty acids and fatty acid ethyl esters can release intracellular Ca^{2+} from intracellular stores, subsequently opening Ca(2+) entry channels in the plasma membrane (*33–36*). It has also been reported that Ca^{2+} influx through voltage-dependent Ca^{2+} channels (VDCCs) causes a rapid halt in mitochondrial movement and induces mitochondrial fragmentation, and this involves activation of Ca^{2+}/calmodulin-dependent protein kinase 1α (CaMKIα) and phosphorylation of Drp1 (*37*). Thus, cellular TG accumulation might be able to regulate mitochondrial morphology through the activation of Ca^{2+}-dependent processes including activation of mitochondrial fission protein Drp1. Additional studies on whether TG accumulation can modulate activities of mitochondrial remodelling proteins including Drp1 will be useful for better understanding of the physiological regulation of mitochondrial remodeling.

We also found that the adipocyte differentiation affected morphology of endoplasmic reticulum (ER) in which morphology of ER was altered from filamentous to fragmented and/or punctate structures as observed in mitochondria (Fig. 5). Although physiological role of changes of ER morphology in adipocyte differentiation is not clear, recent results have shown that Drp1, a mitochondrial fission protein, alters ER-to-mitochondria tethering by causing perinuclear clumping of mitochondria and that Mfn2 is enriched at the ER-mitochondria interface and silencing of Mfn2 disrupts ER morphology and ER-mitochondria interactions (*38–40*). Thus, morphology and functions of ER might be regulated synchronously with those of mitochondria to facilitate proper Ca^{2+} signalling.

Recently, it has been reported that Mfn2 expression is downregulated in skeletal muscle in animal or human obesity and in type 2 diabetic patients (*22*, *23*). Since down-regulation of mitochondrial fusion proteins increased the cellular TG content as described in this study, it can be supposed that cellular TG content in skeletal muscle in these patients was increased compared with healthy control subjects, and thus resulted in the insulin-resistance status. The mitochondrial fusion substances described in this study might be used for the prevention and/or treatment of obesity and type 2 diabetes.

FUNDING

This study was supported by a grant from the Japan Science and Technology Corporation (JST).

CONFLICT OF INTEREST

None declared.

REFERENCES

1. Bereiter-Hahn, J. and Voth, M. (1994) Dynamics of mitochondria in living cells: shape changes, dislocations, fusion, and fission of mitochondria. *Microsc. Res. Technol.* **27**, 198–219
2. Chan, D.C. (2006) Mitochondrial fusion and fission in mammals. *Annu. Rev. Cell Dev. Biol.* **22**, 79–99
3. Hales, K.G. and Fuller, M.T. (1997) Developmentally regulated mitochondrial fusion mediated by a conserved, novel, predicted GTPase. *Cell* **90**, 121–129

4. Rapaport, D., Brunner, M., Neupert, W., and Westermann, B. (1997) Fzo1p is a mitochondrial outer membrane protein essential for the biogenesis of functional mitochondria in Saccharomyces cerevisiae. *J. Biol. Chem.* **273**, 20150–20155
5. Chen, H., Detmer, S., Ewald, A.J., Griffin, E.E., Fraser, S.E., and Chan, D.C. (2003) Mitofusins Mfn1 and Mfn2 coordinately regulate mitochondrial fusion and are essential for embryonic development. *J. Cell Biol.* **160**, 189–200
6. Chen, H., Chomyn, A., and Chan, D.C. (2005) Disruption of fusion results in mitochondrial heterogeneity and dysfunction. *J. Biol. Chem.* **280**, 26185–26192
7. Okamoto, K. and Shaw, J.M. (2005) Mitochondrial morphology and dynamics in yeast and multicellular eukaryotes. *Annu. Rev. Genet.* **39**, 503–506
8. Ishihara, N., Fujita, Y., Oka, T., and Mihara, K. (2006) Regulation of mitochondrial morphology through proteolytic cleavage of OPA1. *EMBO J.* **25**, 2966–2977
9. Alexander, C., Votruba, M., Pesch, U.E., Thiselton, D.L., Mayer, S., Moore, A., Rodriguez, M., Kellner, U., Leo-Kottler, B., Auburger, G., Bhattacharya, S.S., and Wissinger, B. (2000) OPA1, encoding a dynamin-related GTPase, is mutated in autosomal dominant optic atrophy linked to chromosome 3q28. *Nat. Genet.* **26**, 211–215
10. Delettre, C., Lenaers, G., Griffoin, J.M., Gigarel, N., Lorenzo, C., Belenguer, P., Pelloquin, L., Grosgeorge, J., Turc-Carel, C., Perret, E., Astarie-Dequeke, C., Lasquellec, L., Arnaud, B., Ducommun, B., Kaplan, J., and Hamel, C.P. (2000) Nuclear gene OPA1, encoding a mitochondrial dynamin-related protein, is mutated in dominant optic atrophy. *Nat. Genet.* **26**, 207–210
11. Zuchner, S., Mersiyanova, I.V., Muglia, M., Bissar-Tadmouri, N., Rochelle, J., Dadali, E.L., Zappia, M., Nelis, E., Patitucci, A., Senderek, J., Parman, Y., Evgrafov, O., Jonghe, P.D., Takahashi, Y., Tsuji, S., Pericak-Vance, M.A., Quattrone, A., Battologlu, E., Polyakov, A.V., Timmerman, V., Schroder, J.M., and Vance, J.M. (2004) Mutations in the mitochondrial GTPase mitofusin 2 cause Charcot-Marie-Tooth neuropathy type 2A. *Nat. Genet.* **36**, 449–451
12. Kijima, K., Numakura, C., Izumino, H., Umetsu, K., Nezu, A., Shiiki, T., Ogawa, M., Ishizaki, Y., Kitamura, T., Shozawa, Y., and Hayasaka, K. (2005) Mitochondrial GTPase mitofusin 2 mutation in Charcot-Marie-Tooth neuropathy type 2A. *Hum. Genet.* **116**, 23–27
13. Frank, S., Gaume, B., Bergmann-Leitner, E.S., Leitner, W.W., Robert, E.G., Catez, F., Smith, C.L., and Youle, R.J. (2001) The role of dynamin-related protein 1, a mediator of mitochondrial fission, in apoptosis. *Dev. Cell* **1**, 515–525
14. Karbowski, M. and Youle, R.J. (2003) Dynamics of mitochondrial morphology in healthy cells and during apoptosis. *Cell Death Differ.* **10**, 870–880
15. Bossy-Wetzel, E., Barsoum, M.J., Godzik, A., Schwarzenbacher, R., and Lipton, S. (2003) Mitochondrial fission in apoptosis, neurodegeneration and aging. *Curr. Opin. Cell Biol.* **15**, 706–716
16. Olichon, A., Baricault, L., Gas, N., Guillou, E., Valette, A., Belenguer, P., and Lenaers, G. (2003) Loss of OPA1 perturbates the mitochondrial inner membrane structure and integrity, leading to cytochrome c release and apoptosis. *J. Biol. Chem.* **278**, 7743–7746
17. James, D.I., Parone, P.A., Mattenberger, Y., and Martinou, J.C. (2003) hFis1, a novel component of the mammalian mitochondrial fission machinery. *J. Biol. Chem.* **278**, 36373–36379
18. Sugioka, R., Shimizu, S., and Taujimoto, Y. (2004) Fzo1, a protein involved in mitochondrial fusion, inhibits apoptosis. *J. Biol. Chem.* **279**, 52726–52734
19. Arakaki, N., Nishihama, T., Kohda, A., Owaki, H., Kuramoto, Y., Abe, R., Kita, T., Suenaga, M., Himeda, T., Kuwajima, M., Shibata, H., and Higuti, T. (2006) Regulation of mitochondrial morphology and cell survival by Mitogenin I and mitochondrial single-stranded DNA binding protein. *Biochim. Biophys. Acta* **1760**, 1364–1372
20. Li, H., Chen, Y., Jones, A.F., Sanger, R.H., Collis, L.P., Flannery, R., McNay, E.C., Yu, T., Schwarzenbacher, R., Bossy, B., Bossy-Wetzel, E., Bennett, M.V., Pypaert, M., John A. Hickman, J.A., Smith, P.J.S., Hardwick, J.M., and Jonas, E.A. (2008) Bcl-xL induces Drp1-dependent synapse formation in cultured hippocampal neurons. *Proc. Natl Acad. Sci. USA* **105**, 2169–2174
21. Karbowski, M., Norris, K.L., Cleland, M.M., Jeong, S.Y., and Youle, R.J. (2006) Role of Bax and Bak in mitochondrial morphogenesis. *Nature* **443**, 658–662
22. Bach, D., Pich, S., Soriano, F.X., Vega, N., Baumgartner, B., Oriola, J., Daugaard, J.R., Lloberas, J., Camps, M., Zierath, J.R., Rabasa-Lhoret, R., Wallberg-Henriksson, H., Laville, M., Palacín, M., Vidal, H., Rivera, F., Brand, M., and Zorzano, A. (2003) Mitofusin-2 determines mitochondrial network architecture and mitochondrial metabolism. *J. Biol. Chem.* **278**, 17190–17197
23. Bach, D., Naon, D., Pich, S., Soriano, F.X., Vega, N., Rieusset, J., Laville, M., Guillet, C., Boirie, Y., Wallberg-Henriksson, H., Manco, M., Calvani, M., Castagneto, M., Manuel Palacín, M., Mingrone, G., Zierath, J.R., Vidal, H., and Zorzano, A. (2005) Expression of Mfn2, the Charcot-Marie-Tooth neuropathy type 2A gene, in human skeletal muscle: effects of type 2 diabetes, obesity, weight loss, and the regulatory role of tumor necrosis factor alpha and interleukin-6. *Diabetes* **54**, 2685–2693
24. Arakaki, N., Kita, T., Shibata, H., and Higuti, T. (2007) Cell-surface H^+-ATP synthase as potential molecular target for anti-obesity drugs. *FEBS Lett.* **581**, 3405–3409
25. Stone, S.J., Levin, M.C., Zhou, P., Han, J., Walther, T.C., and Farese, R.V. Jr. (2009) The endoplasmic reticulum enzyme DGAT2 is found in mitochondria-associated membranes and has a mitochondrial targeting signal that promotes its association with mitochondria. *J. Biol. Chem.* **284**, 5352–5361
26. Soriano, F.X., Liesa, M., Bach, D., Chan, D.C., Palacin, M., and Zorzano, A. (2006) Evidence for a mitochondrial regulatory pathway defined by peroxisome proliferator-activated receptor-gamma coactivator-1 alpha, estrogen-related receptor-alpha, and mitofusin 2. *Diabetes* **55**, 1783–1791
27. Zheng, J. and Ramirez, V.D. (2000) Inhibition of mitochondrial proton F0F1-ATPase/ATP synthase by polyphenolic phytochemicals. *Br. J. Pharmacol.* **130**, 1115–1123
28. Arakaki, N., Nagao, T., Niki, R., Toyofuku, A., Tanaka, H., Kuramoto, Y., Emoto, Y., Shibata, H., Magota, K., and Higuti, T. (2003) Possible role of cell surface H^+-ATP synthase in the extracellular ATP synthesis and proliferation of human umbilical vein endothelial cells. *Mol. Cancer Res.* **1**, 931–939
29. Skulachev, V.P. (2001) Mitochondrial filaments and clusters as intracellular power-transmitting cables. *Trends Biochem. Sci.* **26**, 23–29
30. Khalimonchuk, O. and Rödel, G. (2005) Biogenesis of cytochrome c oxidase. *Mitochondrion* **5**, 363–388
31. Liu, Z. and Butow, R.A. (2006) Mitochondrial retrograde signaling. *Annu. Rev. Genet.* **40**, 159–185
32. Scarpulla, R.C. (2006) Nuclear control of respiratory gene expression in mammalian cells. *J. Cell Biochem.* **1**, 673–683
33. Criddle, D.N., Raraty, M.G., Neoptolemos, J.P., Tepikin, A.V., Petersen, O.H., and Sutton, R. (2004) Ethanol toxicity in pancreatic acinar cells: mediation by nonoxidative fatty acid metabolites. *Proc. Natl Acad. Sci. USA* **101**, 10738–10743
34. Zhang, H.M., Dang, H., Yeh, C.K., and Zhang, B.X. (2009) Linoleic acid-induced mitochondrial Ca^{2+} efflux causes peroxynitrite generation and protein nitrotyrosylation. *PLoS One* **4**, 1–10

35. Gerasimenko, J.V., Lur, G., Sherwood, M.W., Ebisui, E., Tepikin, A.V., Mikoshiba, K., Gerasimenko, O.V., and Petersen, O.H. (2009) Pancreatic protease activation by alcohol metabolite depends on Ca^{2+} release via acid store IP_3 receptor. *Proc. Natl Acad. Sci. USA* **106**, 10758–10763
36. Guo, W., Wong, S., Xie, W., Lei, T., and Luo, Z. (2007) Palmitate modulates intracellular signaling, induces endoplasmic reticulum stress, and causes apoptosis in mouse 3T3-L1 and rat primary preadipocytes. *Am. J. Physiol. Endocrinol. Metab.* **293**, E576–E586
37. Han, X.J., Lu, Y.F., Li, S.A., Kaitsuka, T., Sato, Y., Tomizawa, K., Nairn, A.C., Takei, K., Matsui, H., and Matsushita, M. (2008) CaM kinase Iα-induced phosphorylation of Drp1 regulates mitochondrial morphology. *J. Cell Biol.* **182**, 573–585
38. Pitts, K.R., Yoon, Y., Krueger, E.W., and McNiven, M.A. (1999) The dynamin-like protein DLP1 is essential for normal distribution and morphology of the endoplasmic reticulum and mitochondria in mammalian cells. *Mol. Biol. Cell* **10**, 4403–4417
39. Szabadkai, G., Bianchi, K., Varnai, P., De Stefani, D., Wieckowski, M.R., Cavagna, D., Nagy, A.I., Balla, T., and Rizzuto, R. (2006) Chaperone-mediated coupling of endoplasmic reticulum and mitochondrial Ca^{2+} channels. *J. Cell Biol.* **175**, 901–911
40. de Brito1, O.M. and Scorrano, L. (2008) Mitofusin 2 tethers endoplasmic reticulum to mitochondria. *Nature* **456**, 605–611